PARTICLE ASTROPHYSICS

Extended gamma-ray sources around pulsars constrain the origin of the positron flux at Earth

A. U. Abeysekara,[1] A. Albert,[2] R. Alfaro,[3] C. Alvarez,[4] J. D. Álvarez,[5] R. Arceo,[4] J. C. Arteaga-Velázquez,[5] D. Avila Rojas,[3] H. A. Ayala Solares,[6] A. S. Barber,[1] N. Bautista-Elivar,[7] A. Becerril,[3] E. Belmont-Moreno,[3] S. Y. BenZvi,[8] D. Berley,[9] A. Bernal,[10] J. Braun,[11] C. Brisbois,[6] K. S. Caballero-Mora,[4] T. Capistrán,[12] A. Carramiñana,[12] S. Casanova,[13,14] M. Castillo,[5] U. Cotti,[5] J. Cotzomi,[15] S. Coutiño de León,[12] C. De León,[15] E. De la Fuente,[16] B. L. Dingus,[2] M. A. DuVernois,[11] J. C. Díaz-Vélez,[16] R. W. Ellsworth,[17] K. Engel,[9] O. Enríquez-Rivera,[18] D. W. Fiorino,[9] N. Fraija,[10] J. A. García-González,[3] F. Garfias,[10] M. Gerhardt,[6] A. González Muñoz,[3] M. M. González,[10] J. A. Goodman,[9] Z. Hampel-Arias,[11] J. P. Harding,[2] S. Hernández,[3] A. Hernández-Almada,[3] J. Hinton,[14] B. Hona,[6] C. M. Hui,[19] P. Hüntemeyer,[6] A. Iriarte,[10] A. Jardin-Blicq,[14] V. Joshi,[14] S. Kaufmann,[4] D. Kieda,[1] A. Lara,[18] R. J. Lauer,[20] W. H. Lee,[10] D. Lennarz,[21] H. León Vargas,[3] J. T. Linnemann,[22] A. L. Longinotti,[12] G. Luis Raya,[7] R. Luna-García,[23] R. López-Coto,[14]* K. Malone,[24] S. S. Marinelli,[22] O. Martinez,[15] I. Martinez-Castellanos,[9] J. Martínez-Castro,[23] H. Martínez-Huerta,[25] J. A. Matthews,[20] P. Miranda-Romagnoli,[26] E. Moreno,[15] M. Mostafá,[24] L. Nellen,[27] M. Newbold,[1] M. U. Nisa,[8] R. Noriega-Papaqui,[26] R. Pelayo,[23] J. Pretz,[24] E. G. Pérez-Pérez,[7] Z. Ren,[20] C. D. Rho,[8] C. Rivière,[9] D. Rosa-González,[12] M. Rosenberg,[24] E. Ruiz-Velasco,[3] H. Salazar,[15] F. Salesa Greus,[13]* A. Sandoval,[3] M. Schneider,[28] H. Schoorlemmer,[14] G. Sinnis,[2] A. J. Smith,[9] R. W. Springer,[1] P. Surajbali,[14] I. Taboada,[21] O. Tibolla,[4] K. Tollefson,[22] I. Torres,[12] T. N. Ukwatta,[2] G. Vianello,[29] T. Weisgarber,[11] S. Westerhoff,[11] I. G. Wisher,[11] J. Wood,[11] T. Yapici,[22] G. Yodh,[30] P. W. Younk,[2] A. Zepeda,[25,4] H. Zhou,[2]* F. Guo,[2] J. Hahn,[14] H. Li,[2] H. Zhang[2]

The unexpectedly high flux of cosmic-ray positrons detected at Earth may originate from nearby astrophysical sources, dark matter, or unknown processes of cosmic-ray secondary production. We report the detection, using the High-Altitude Water Cherenkov Observatory (HAWC), of extended tera–electron volt gamma-ray emission coincident with the locations of two nearby middle-aged pulsars (Geminga and PSR B0656+14). The HAWC observations demonstrate that these pulsars are indeed local sources of accelerated leptons, but the measured tera–electron volt emission profile constrains the diffusion of particles away from these sources to be much slower than previously assumed. We demonstrate that the leptons emitted by these objects are therefore unlikely to be the origin of the excess positrons, which may have a more exotic origin.

Cosmic rays are high-energy particles from space that have been known for more than a century. The origin of high-energy cosmic rays and how they are accelerated remains unclear. Most cosmic rays are protons or atomic nuclei, but positrons and electrons also are a small fraction of the total cosmic-ray flux. Positrons are especially puzzling because the PAMELA (Payload for Antimatter Matter Exploration and Light-nuclei Astrophysics) detector observed an unexpected excess of positrons at energies >10 GeV, compared with the predicted flux that originates from interactions of cosmic-ray protons propagating through the Galaxy (*1*). Confirmation of these results has come from the Fermi Large Area Telescope (*2*) and AMS [Alpha Magnetic Spectrometer (*3*)] experiments; the latter also showed that the excess signal extends to hundreds of giga–electron volts.

Energy losses experienced in interstellar magnetic and radiation fields by the highest-energy positrons require that their sources lie within a few hundred parsecs from Earth (*4*). Nearby potential cosmic-ray accelerators—for example, pulsar wind nebulae (PWNe)—have been proposed as the sources of these extra positrons (*5*, *6*). A PWN consists of a rapidly spinning neutron star (pulsar) that produces a wind of electrons and positrons that are further accelerated by the surrounding shock with the interstellar medium (ISM). There are a handful of known pulsars that are both close enough to be candidate sources and sufficiently old for the highest-energy positrons to have had time to arrive at Earth (*7*, *8*). Nearby dark matter particle interactions could also produce positrons (*9*). Both PWNe and dark matter sources should also produce gamma rays that could potentially be observed coming from the sources, unlike positrons (whose paths are deflected by magnetic fields).

Recently, the High-Altitude Water Cherenkov Observatory (HAWC) collaboration reported the detection of tera–electron volt gamma rays around two nearby pulsars, which are among those proposed to produce the local positrons (*10*). HAWC is a wide-field-of-view, continuously operating detector of extensive air showers initiated by gamma rays and cosmic rays interacting in the atmosphere (*11*). The angular resolution improves from 1.0° to 0.2° with the size of the air shower. HAWC is the most sensitive survey detector above 10 TeV and is well suited to detecting nearby sources, which would have a greater angular extent. Operation of the full detector began in March 2015, and the data set presented here includes 507 days, as described in (*11*).

Tera–electron volt gamma-ray emissions from the pulsars Geminga and PSR B0656+14 were found in a search for extended sources that was performed for the HAWC catalog, in which these two pulsars have the designations 2HWC J0635+180 and 2HWC J0700+143 (*10*). By fitting to a diffusion model (*12*), the two sources were detected with a significance at the pulsar location of 13.1 and 8.1 standard deviations (σ), respectively (Fig. 1A). The tera–electron volt emission region is several degrees across, which we attribute to electrons and positrons diffusing away from the

[1]Department of Physics and Astronomy, University of Utah, Salt Lake City, UT, USA. [2]Los Alamos National Laboratory, Los Alamos, NM, USA. [3]Instituto de Física, Universidad Nacional Autónoma de México, Mexico City, Mexico. [4]Universidad Autónoma de Chiapas, Tuxtla Gutiérrez, Chiapas, Mexico. [5]Universidad Michoacana de San Nicolás de Hidalgo, Morelia, Mexico. [6]Department of Physics, Michigan Technological University, Houghton, MI, USA. [7]Universidad Politecnica de Pachuca, Pachuca, Hidalgo, Mexico. [8]Department of Physics and Astronomy, University of Rochester, Rochester, NY, USA. [9]Department of Physics, University of Maryland, College Park, MD, USA. [10]Instituto de Astronomía, Universidad Nacional Autónoma de México, Mexico City, Mexico. [11]Department of Physics, University of Wisconsin–Madison, Madison, WI, USA. [12]Instituto Nacional de Astrofísica, Óptica y Electrónica, Puebla, Mexico. [13]Institute of Nuclear Physics Polish Academy of Sciences, Krakow, Poland. [14]Max-Planck Institute for Nuclear Physics, Heidelberg, Germany. [15]Facultad de Ciencias Físico Matemáticas, Benemérita Universidad Autónoma de Puebla, Puebla, Mexico. [16]Departamento de Física, Centro Universitario de Ciencias Exactas e Ingenierías, Universidad de Guadalajara, Guadalajara, Mexico. [17]School of Physics, Astronomy, and Computational Sciences, George Mason University, Fairfax, VA, USA. [18]Instituto de Geofísica, Universidad Nacional Autónoma de México, Mexico City, Mexico. [19]Astrophysics Office, NASA Marshall Space Flight Center Huntsville, AL, USA. [20]Department of Physics and Astronomy, University of New Mexico, Albuquerque, NM, USA. [21]School of Physics and Center for Relativistic Astrophysics, Georgia Institute of Technology, Atlanta, GA, USA. [22]Department of Physics and Astronomy, Michigan State University, East Lansing, MI, USA. [23]Centro de Investigación en Computación, Instituto Politécnico Nacional, Mexico City, Mexico. [24]Department of Physics, Pennsylvania State University, University Park, PA, USA. [25]Physics Department, Centro de Investigacion y de Estudios Avanzados del IPN, Mexico City, Mexico. [26]Universidad Autónoma del Estado de Hidalgo, Pachuca, Mexico. [27]Instituto de Ciencias Nucleares, Universidad Nacional Autónoma de México, Mexico City, Mexico. [28]Santa Cruz Institute for Particle Physics, University of California, Santa Cruz, Santa Cruz, CA, USA. [29]Hansen Experimental Physics Laboratory Stanford University, Stanford, CA, USA. [30]Department of Physics and Astronomy, University of California, Irvine, Irvine, CA, USA.
*Corresponding author. Email: rlopez@mpi-hd.mpg.de (R.L.-C.); francisco.salesa@ifj.edu.pl (F.S.G.); hao@lanl.gov (H.Z.)

pulsar and up-scattering the cosmic microwave background (CMB) photons. Geminga was previously detected at tera–electron volt energies by the Milagro observatory, with a flux and angular extent consistent with the HAWC observation but with lower statistical significance (*13*). Here we show that the HAWC observation of the spectral and spatial properties of these sources can be used to constrain their contribution to the positron flux at Earth (Fig. 1B).

A diffusion model of the spatial and spectral morphology (*12*) is fit to the gamma-ray flux N as a function of angle θ from the source and gamma-ray energy E as

$$\frac{d^2N}{dEd\Omega} = N_0\left(\frac{E}{20\text{TeV}}\right)^{-\alpha} \times \frac{1.22}{\pi^{3/2}\theta_d(E)[\theta + 0.06\theta_d(E)]} e^{\left[-\theta^2/\theta_d(E)^2\right]} \quad (1)$$

using a maximum likelihood technique. N_0 is the flux normalization at 20 TeV, and Ω denotes a solid angle. The diffusion angle θ_d is proportional to the square root of the diffusion coefficient D, and both vary with energy. The model values from the fit are given in Table 1. The spectral indices α and observed fluxes are similar to those of other tera–electron volt PWNe (*14*), but the luminosities are lower, primarily because of their nearby distance and larger apparent size. The energy range is estimated by increasing (decreasing) the minimum (maximum) energy of an abrupt cutoff in the power law spectrum until the significance of the fit decreases by 1σ.

Assuming that all the observed gamma-ray emission at tera–electron volt energies is produced

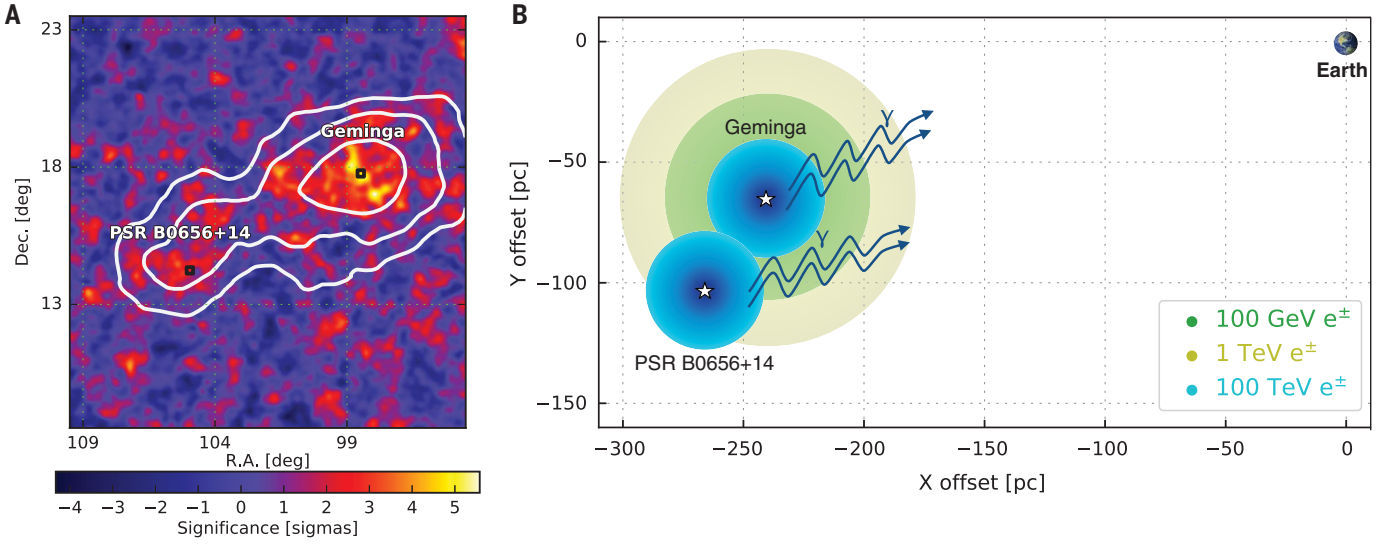

Fig. 1. Spatial morphology of Geminga and PSR B0656+14. (**A**) HAWC significance map (between 1 and 50 TeV) for the region around Geminga and PSR B0656+14, convolved with the HAWC point spread function and with contours of 5σ, 7σ, and 10σ for a fit to the diffusion model. R.A., right ascension; dec., declination. (**B**) Schematic illustration of the observed region and Earth, shown projected onto the Galactic plane. The colored circles correspond to the diffusion distance of leptons with three different energies from Geminga; for clarity, only the highest energy (blue) is shown for PSR B0656+14. The balance between diffusion rate and cooling effects means that tera–electron volt particles diffuse the farthest (fig. S1).

Table 1. Pulsar parameters, values of parameters from the model fitting to the observed extended gamma-ray emission, and assumed parameters of our model. Pulsar parameters are from (*15*).

		Geminga	PSR B0656+14
Pulsar parameters			
(Right ascension, declination) (J2000 source location)	(degrees)	(98.48, 17.77)	(104.95, 14.24)
τ_c (characteristic age)	(years)	342,000	110,000
T (spin period)	(seconds)	0.237	0.385
d (distance)	(parsecs)	250^{+120}_{-62}	288^{+33}_{-27}
dE/dt (energy loss rate due to pulsar's spin slowing)	($\times 10^{34}$ ergs per second)	3.26	3.8
Model values			
θ_0 (θ_d for 20-TeV gamma ray)	(degrees)	5.5 ± 0.7	4.8 ± 0.6
N_0	($\times 10^{-15}$ photons per tera–electron volt per square centimeter per second)	$13.6^{+2.0}_{-1.7}$	$5.6^{+2.5}_{-1.7}$
α		2.34 ± 0.07	2.14 ± 0.23
D_{100} (diffusion coefficient of 100-TeV electrons from joint fit of two PWNe)	($\times 10^{27}$ square centimeters per second)	4.5 ± 1.2	4.5 ± 1.2
D_{100} (diffusion coefficient of 100-TeV electrons from individual fit of PWN)	($\times 10^{27}$ square centimeters per second)	$3.2^{+1.4}_{-1.0}$	15^{+49}_{-9}
Energy range	(tera–electron volt)	8 to 40	8 to 40
Luminosity in gamma rays over this energy range	($\times 10^{31}$ ergs per second)	11 × $(d/250\ \text{pc})^2$	4.5 × $(d/288\ \text{pc})^2$
Assumed parameters			
L_0 (initial spin-down power)	($\times 10^{36}$ ergs per second)	27.8	4.0
W_e (total energy released since pulsar's birth)	($\times 10^{48}$ ergs)	11.0	1.5

by relativistic electron and positron pairs, we calculate the electron and positron flux produced by these sources at Earth. Tera–electron volt gamma rays are produced when positrons or electrons inverse Compton scatter lower-energy photons to higher energies. Gamma rays at ~20 TeV are produced by electrons and positrons at ~100 TeV (*12*). At these energies, the scattered photons are primarily from the CMB, because the cross section for scattering higher-energy infrared and optical photons is strongly suppressed.

Charged particles also lose energy by synchrotron radiation when propagating through a magnetic field. At the nominal distances of Geminga and PSR B0656+14 at 250 and 288 pc, respectively (*15*), the observed spatial extent of these two sources at tera–electron volt energies is tens of parsecs, which is much greater than the <0.1 pc nebula observed in x-rays (*16*, *17*). The x-ray emission is from synchrotron radiation, where the magnetic field is enhanced by the pulsar to 10 to 20 μG (*18*). The region emitting tera–electron volt gamma rays is primarily outside the x-ray nebula, so we assume that the magnetic field is equal to that of the nearby ISM at 3 μG (*19*) and is not increased by the presence of the pulsar or the prior supernova remnant. The implied energy density of the particles accelerated by the pulsar is several orders of magnitude less than the energy density of the interstellar magnetic fields, so the particles themselves do not amplify the field. If the magnetic field was higher, the pulsar could not provide enough energy to produce the observed gamma-ray luminosity.

We assume that particles are accelerated from 1 GeV to 500 TeV with a power-law energy spectrum. The spectral index of the electrons is chosen to fit the HAWC gamma-ray observations and is harder than the gamma-ray spectra by ~0.1 (*12*). The total flux of electrons and positrons is 40 and 4% of the measured power released by the slowing of the spin of Geminga and PSR B0656+14, respectively. Because most of the power released is in electrons with energies below those measured by HAWC, the conversion of the spin-down power to accelerated electrons could be less efficient if the spectrum breaks at lower energies. However, lower efficiencies reduce the local positron flux. The tera–electron volt gamma rays could also be produced by high-energy protons interacting with matter. However, the matter density around these sources is low (*20*), and a proton origin of the gamma-ray emission is disfavored because the required power would be even larger than the total energy injected by the pulsar.

If electrons and positrons are injected continuously and diffuse isotropically away from their sources, the density of particles is proportional to $(1/r)\mathrm{erfc}(r/r_\mathrm{d})$, where r_d is the diffusion radius, r is the distance from the pulsar, and erfc is the error function (*21*). The integral of this function along the line of sight is the gamma-ray surface brightness. The diffusion radius is defined as $r_\mathrm{d} = 2\sqrt{D\,t}$; here, D is the diffusion coefficient, and t is the lepton injection time and is chosen to be the electron-cooling time for the energy of electrons that produce the HAWC observation (*12*). The diffusion coefficient increases with energy E as E^δ, where δ is chosen to be 1/3, motivated by the Kolmogorov turbulence model (*22*). This value of δ is also compatible with recent results from AMS-02 for the spectrum of hadronic cosmic rays that are produced by spallation (*23*).

The observed surface brightness distributions of Geminga and PSR B0656+14 are shown in Fig. 2, along with our model fit. The fitted values of D_{100} (where D_{100} is the diffusion coefficient for electrons at 100 TeV) are given in Table 1. Because the sources are close to each other spatially, as seen in Fig. 1, we also fit a single D_{100} to both (Table 1). The values of D_{100} derived from a joint fit and fits to the individual sources are equivalent within the uncertainties. We also fit the emission around Geminga with an elongated diffusion model, and the fit result is not statistically significant over the isotropic diffusion model, so there is no evidence of anisotropic diffusion in these data.

The value of D_{100} derived from our HAWC observations ($4.5 \pm 1.2 \times 10^{27}$ cm^2 s^{-1}) is smaller by a factor of about 100 than those considered in previous models of electron diffusion into the local ISM (*5*–*8*, *24*). These other models assumed that D was similar to the value inferred from hadronic cosmic rays, which may not be applicable to positrons in the local ISM. Spatial inhomogeneities are possible (*25*), and such a low D could arise from additional effects of turbulent scattering (*26*, *27*), for example. Because the angular extent of the tera–electron volt source is proportional to $\sqrt{D_{100}}$, a diffusion coefficient larger by a factor of 100 would result in an angular extent for the source that is larger by a factor of 10 and a surface brightness for the same total flux that is smaller by a factor of 100. This would make these two sources undetectable by HAWC.

To calculate the positrons that have diffused to Earth, the history of the pulsar's emission must be included because the lifetime of sub-tera–electron volt positrons in the ISM can exceed that of the pulsar. Assuming that a pulsar is a pure dipole radiator and hence has a braking index of 3, its luminosity L at a time t after its birth is predicted to vary as $L = L_0(1 + t/\tau)^{-2}$. We take the characteristic initial pulsar spin-down time scale (τ) of 12,000 years for Geminga (*28*) and assume it to be the same for PSR B0656+14. The electron transport equation is solved using the EDGE code (*29*) for electron diffusion (*12*).

Figure 3 shows the expected flux of positrons as a function of energy from Geminga (blue line) compared with the measured flux of positrons by AMS-02 in low Earth orbit. The positron flux from Geminga exceeds by several orders of magnitude

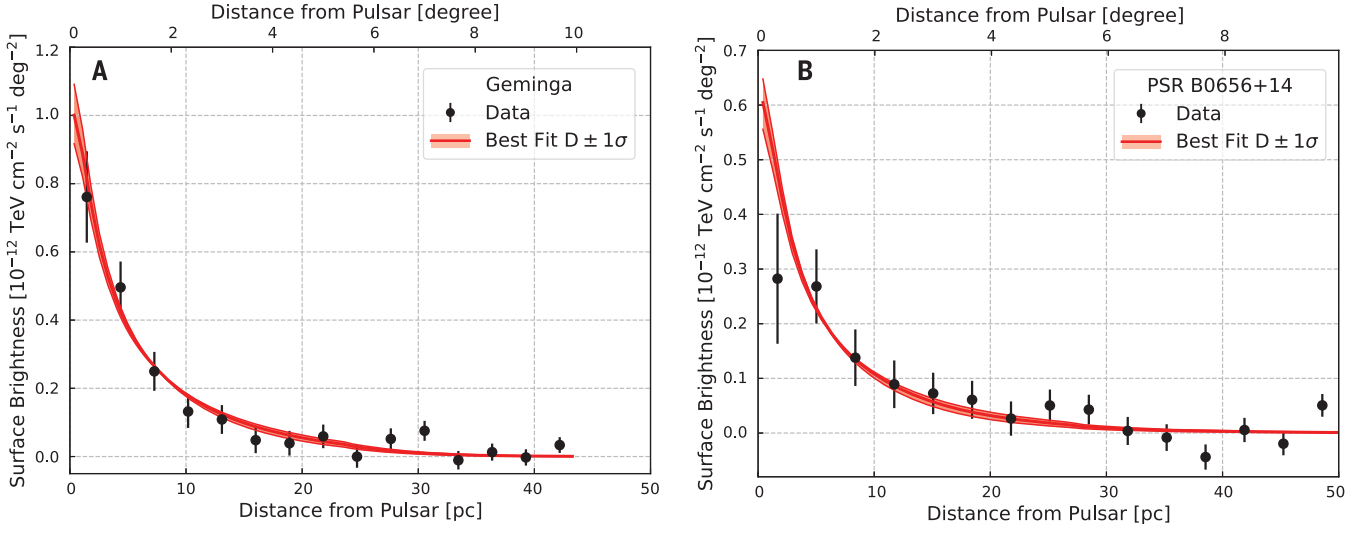

Fig. 2. Surface brightness of the tera–electron volt gamma-ray emission. Surface brightness is shown as a function of distance from the Geminga (**A**) and PSR B0656+14 (**B**) pulsars. The solid line represents the best-fitting model with a common diffusion coefficient, and the shaded band is the ±1σ statistical uncertainty. Error bars are statistical errors. The distance from each pulsar in parsecs is calculated based on nominal distances of 250 and 288 pc for Geminga and PSR B0656+14, respectively (*14*).

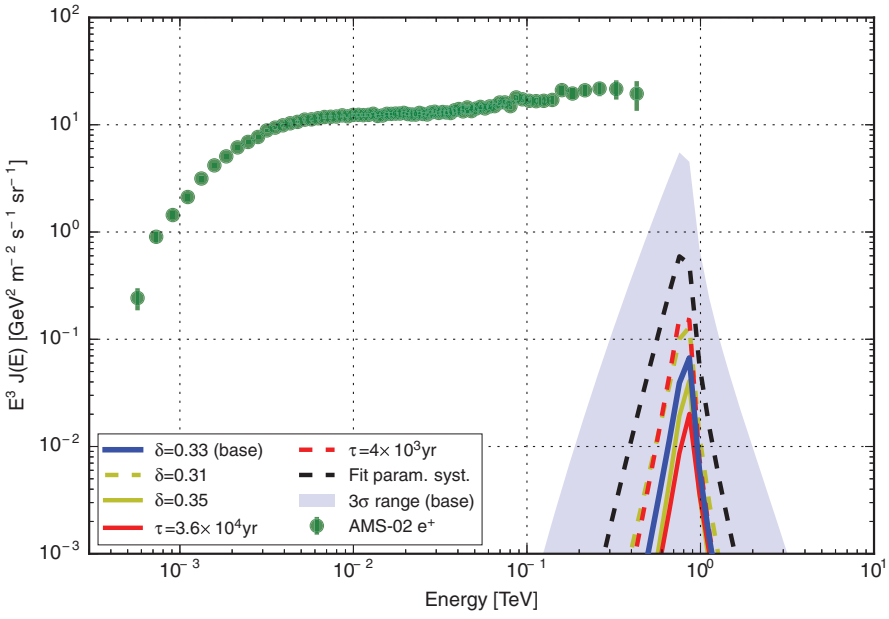

Fig. 3. Estimated positron energy flux at Earth from Geminga (blue solid line), compared with AMS-02 experimental measurements (green dots). The shaded blue region indicates the 3σ (99.5% confidence) statistical uncertainty from simulations (*12*). Additional lines represent the effect on the positron energy flux of varying several systematic effects: the pulsar characteristic initial spin-down time scale (red lines); the index of the diffusion coefficient (yellow lines); and the diffusion angle, spectral index of the injected electrons, and flux normalization combined (black line). The spectrum expected at Earth is strongly peaked at the energy where the cooling time equals the age of the pulsar. The positron flux at Earth from PSR B0656+14 is several orders of magnitude lower than that from Geminga and below the range of this plot. AMS-02 experimental measurements are from (*34*); error bars come from the quadratic sum of statistical and systematic errors. Both AMS-02 experimental measurements and error values were fetched from an online database (*35*).

that from PSR B0656+14, owing to the combination of Geminga's greater gamma-ray flux that injects more energy into electrons, its older age, and its closer distance. We consider the impact of different systemic effects (*12*): If the spectral index of the diffusion coefficient δ were smaller, lower-energy positrons would diffuse faster; if the characteristic initial spin-down time scale τ were shorter, the luminosity would have been higher in the past. If the current distance were smaller, that would not change the local positron flux substantially because the true D_{100} would also have to be smaller (because it is derived from the angular extent of the sources). Therefore, in this model, these pulsars do not produce a measurable contribution to the positron flux measured by AMS-02 at Earth. Moreover, regardless of the absolute flux, their strongly peaked energy spectrum is incompatible with the flat distribution in energy found by AMS-02.

Our conclusions conflict with a recent estimate (*30*) based on the HAWC catalog data (*10*). The model in (*30*) considers the effect of constant-velocity convective winds to be dominant over diffusion. We have shown here that the tera–electron volt gamma-ray surface brightness measured by HAWC—not available at the time of publication of (*30*)—is well fit by a diffusion profile and strongly disfavors the convection profile. Moreover, the absence of any pressure or energy source to power this strong wind strongly disfavors the model in (*30*) and the conclusions drawn regarding the local positron flux.

Geminga and PSR B0656+14 are the oldest pulsars for which a tera–electron volt nebula has so far been detected. Under our assumption of isotropic and homogeneous diffusion, the dominant source of the positron flux above 10 GeV cannot be either Geminga or PSR B0656+14. Under the unlikely situation that the field is nearly aligned along the direction between Earth and the nearby tera–electron volt nebulae, the local positron flux can be increased; however, the tera–electron volt morphology of the sources matches our isotropic diffusion model. We therefore favor the explanation that instead of these two pulsars, the origin of the local positron flux must be explained by other processes, such as different assumptions about secondary production [although that has been questioned (*31*, *32*)], other pulsars, other types of cosmic accelerators such as microquasars (*33*) and supernova remnants (*32*), or the annihilation or decay of dark matter particles (*9*).

REFERENCES AND NOTES

1. O. Adriani *et al.*, *Nature* **458**, 607–609 (2009).
2. Fermi LAT Collaboration, *Phys. Rev. Lett.* **108**, 011103 (2012).
3. AMS Collaboration, *Phys. Rev. Lett.* **113**, 121101 (2014).
4. I. V. Moskalenko, A. W. Strong, *Astrophys. J.* **493**, 694–707 (1998).
5. D. Hooper, P. Blasi, P. D. Serpico, *J. Cosmol. Astropart. Phys.* **2009**, 025 (2009).
6. T. Delahaye, J. Lavalle, R. Lineros, F. Donato, N. Fornengo, *Astron. Astrophys.* **524**, A51 (2010).
7. P.-F. Yin, Z.-H. Yu, Q. Yuan, X.-J. Bi, *Phys. Rev. D Part. Fields Gravit. Cosmol.* **88**, 023001 (2013).
8. S. Profumo, *Cent. Eur. J. Phys.* **10**, 1–31 (2011).
9. A. Ibarra, A. S. Lamperstorfer, J. Silk, *Phys. Rev. D* **89**, 063539 (2014).
10. A. U. Abeysekara *et al.*, *Astrophys. J.* **843**, 21 (2017).
11. A. U. Abeysekara *et al.*, *Astrophys. J.* **843**, 17 (2017).
12. Materials and methods are available as supplementary materials.
13. A. A. Abdo *et al.*, *Astrophys. J.* **664**, L91–L94 (2007).
14. H.E.S.S. collaboration, The population of TeV pulsar wind nebulae in the H.E.S.S. Galactic Plane Survey. arXiv:1702.08280 [astro-ph.HE] (27 February 2017).
15. R. N. Manchester, G. B. Hobbs, A. Teoh, M. Hobbs, *Astron. J.* **129**, 1993–2006 (2005).
16. P. A. Caraveo *et al.*, *Science* **301**, 1345–1347 (2003).
17. B. Posselt *et al.*, *Astrophys. J.* **835**, 66 (2017).
18. L. Bîrzan, G. G. Pavlov, O. Kargaltsev, *Astrophys. J.* **817**, 129 (2016).
19. A. H. Minter, S. R. Spangler, *Astrophys. J.* **458**, 194–214 (1996).
20. F. Paresce, *Astron. J.* **89**, 1022–1037 (1984).
21. A. M. Atoyan, F. A. Aharonian, H. J. Völk, *Phys. Rev. D* **52**, 3265–3275 (1995).
22. A. N. Kolmogorov, *Dokl. Akad. Nauk SSSR* **30**, 301–305 (1941).
23. AMS Collaboration, *Phys. Rev. Lett.* **117**, 231102 (2016).
24. H. Yüksel, M. D. Kistler, T. Stanev, *Phys. Rev. Lett.* **103**, 051101 (2009).
25. G. Jóhannesson *et al.*, *Astrophys. J.* **824**, 16 (2016).
26. H. Yan, A. Lazarian, *Astrophys. J.* **614**, 757–769 (2004).
27. M. A. Malkov, P. H. Diamond, R. Z. Sagdeev, F. A. Aharonian, I. V. Moskalenko, *Astrophys. J.* **768**, 73 (2013).
28. F. A. Aharonian, M. A. Atoyan, J. H. Völk, *Astron. Astrophys.* **294**, L41–L44 (1995).
29. R. Lopez-Coto *et al.*, arXiv:1708.03139 [astro-ph.HE] (10 August 2017).
30. D. Hooper, I. Cholis, T. Linden, K. Fang, arXiv:1702.08436 [astro-ph.HE] (27 February 2017).
31. I. Cholis, D. Hooper, *Phys. Rev. D* **89**, 043013 (2014).
32. M. A. Malkov, P. H. Diamond, R. Z. Sagdeev, *Phys. Rev. D* **94**, 063006 (2016).
33. N. Gupta, D. F. Torres, *Mon. Not. R. Astron. Soc.* **441**, 3122–3126 (2014).
34. AMS Collaboration, *Phys. Rev. Lett.* **113**, 121102 (2014).
35. D. Maurin, F. Melot, R. Taillet, *Astron. Astrophys.* **569**, A32.

ACKNOWLEDGMENTS

We acknowledge the support from the U.S. National Science Foundation (NSF); the U.S. Department of Energy Office of High-Energy Physics; the Laboratory Directed Research and Development program of Los Alamos National Laboratory; Consejo Nacional de Ciencia y Tecnología, México (grants 271051, 232656, 260378, 179588, 239762, 254964, 271737, 258865, 243290, 132197, and 281653) (Cátedras 873, 1563); Laboratorio Nacional HAWC de rayos gamma; L'Oreal Fellowship for Women in Science 2014; Red HAWC, México; DGAPA-UNAM (Dirección General Asuntos del Personal Académico–Universidad Nacional Autónoma de México; grants IG100317, IN111315, IN111716-3, IA102715, 109916, and IA102917); VIEP-BUAP (Vicerrectoría de Investigación y Estudios de Posgrado–Benemérita Universidad Autónoma de Puebla); PIFI (Programa Integral de Fortalecimiento Institucional) 2012 and 2013; PROFOCIE (Programa de Fortalecimiento de la Calidad en Instituciones Educativas) 2014 and 2015; the University of Wisconsin Alumni Research Foundation; the Institute of Geophysics, Planetary Physics, and Signatures at Los Alamos National Laboratory; Polish Science Centre grant DEC-2014/13/B/ST9/945; and Coordinación de la Investigación Científica de la Universidad Michoacana. Thanks to S. Delay, L. Díaz, and E. Murrieta for technical support. The data and software to reproduce Figs. 1 to 3 and the values of the gamma-ray flux parameters in Table 1 are available at https://data.hawc-observatory.org/datasets/geminga2017/.

SUPPLEMENTARY MATERIALS

www.sciencemag.org/content/358/6365/911/suppl/DC1
Materials and Methods
Figs. S1 and S2
Table S1
References (*36*–*41*)

20 April 2017; accepted 9 October 2017
10.1126/science.aan4880

Extended gamma-ray sources around pulsars constrain the origin of the positron flux at Earth

A. U. Abeysekara, A. Albert, R. Alfaro, C. Alvarez, J. D. Álvarez, R. Arceo, J. C. Arteaga-Velázquez, D. Avila Rojas, H. A. Ayala Solares, A. S. Barber, N. Bautista-Elivar, A. Becerril, E. Belmont-Moreno, S. Y. BenZvi, D. Berley, A. Bernal, J. Braun, C. Brisbois, K. S. Caballero-Mora, T. Capistrán, A. Carramiñana, S. Casanova, M. Castillo, U. Cotti, J. Cotzomi, S. Coutiño de León, C. De León, E. De la Fuente, B. L. Dingus, M. A. DuVernois, J. C. Díaz-Vélez, R. W. Ellsworth, K. Engel, O. Enríquez-Rivera, D. W. Fiorino, N. Fraija, J. A. García-González, F. Garfias, M. Gerhardt, A. González Muñoz, M. M. González, J. A. Goodman, Z. Hampel-Arias, J. P. Harding, S. Hernández, A. Hernández-Almada, J. Hinton, B. Hona, C. M. Hui, P. Hüntemeyer, A. Iriarte, A. Jardin-Blicq, V. Joshi, S. Kaufmann, D. Kieda, A. Lara, R. J. Lauer, W. H. Lee, D. Lennarz, H. León Vargas, J. T. Linnemann, A. L. Longinotti, G. Luis Raya, R. Luna-García, R. López-Coto, K. Malone, S. S. Marinelli, O. Martinez, I. Martinez-Castellanos, J. Martínez-Castro, H. Martínez-Huerta, J. A. Matthews, P. Miranda-Romagnoli, E. Moreno, M. Mostafá, L. Nellen, M. Newbold, M. U. Nisa, R. Noriega-Papaqui, R. Pelayo, J. Pretz, E. G. Pérez-Pérez, Z. Ren, C. D. Rho, C. Rivière, D. Rosa-González, M. Rosenberg, E. Ruiz-Velasco, H. Salazar, F. Salesa Greus, A. Sandoval, M. Schneider, H. Schoorlemmer, G. Sinnis, A. J. Smith, R. W. Springer, P. Surajbali, I. Taboada, O. Tibolla, K. Tollefson, I. Torres, T. N. Ukwatta, G. Vianello, T. Weisgarber, S. Westerhoff, I. G. Wisher, J. Wood, T. Yapici, G. Yodh, P. W. Younk, A. Zepeda, H. Zhou, F. Guo, J. Hahn, H. Li and H. Zhang

Science **358** (6365), 911-914.
DOI: 10.1126/science.aan4880

Exotic origin for cosmic positrons

Several cosmic-ray detectors have found more positrons arriving at Earth than expected. Some researchers interpret this as a signature of exotic physics, such as the annihilation of dark matter particles. Others prefer a more mundane explanation that involves positron generation at pulsars followed by diffusion to Earth. Abeysekara *et al.* detected extended emission of gamma rays around two nearby pulsars, generated by high-energy electrons and positrons. The size of the extended emission was used to calculate how far positrons generated by the pulsars diffuse through space—which turns out to be insufficient to reach Earth. The excess positrons detected on Earth must therefore have a more exotic origin than nearby pulsars.

Science, this issue p. 911